Multiscale Modeling of Stress-Mediated Diffusion in Silicon - Ab Initio to Continuum

W. Windl[*], M. Laudon[**] , M. S. Daw[*], N. N. Carlson[**], and M. P. Masquelier[**]

Computational Materials, Motorola, Inc.
[*]Austin, TX, USA
[**]Los Alamos, NM, USA
Wolfgang.Windl@Motorola.com

ABSTRACT

The introduction of new "back-end" materials, as well as the further scaling of silicon device dimensions, has raised the level of stress in device structures. Current engineering simulations of diffusion neglect the direct effect of stress on diffusivity. In this paper, we demonstrate for the first time the development of a complete methodology to simulate the effects of general anisotropic non-uniform stress on diffusion of B in Si. The macroscopic diffusion equation is derived from microscopic transition state theory, relating the diffusivity to the microscopic jump parameters. The required microscopic parameters are calculated from first principles. Stress in gate stack materials is measured as a function of temperature and used to develop a stress-prediction methodology. All these numbers are implemented into a continuum model and used to examine diffusion in a complex stress field.

Keywords: Multiscale modeling, stress-mediated diffusion, ab-initio, continuum.

1 INTRODUCTION

Traditionally, it has been assumed that substrate stresses were directly coupled with dislocation formation and response [1,2], whereas stress effects on diffusion were thought to be negligible [3]. This assumption has typically been valid due to relatively low stress values in the gate material (poly-silicon on silicon) and because the resulting modifications in the dopant profile due to stress were relatively small compared to the gate length. As gate lengths reduce in size and as more exotic materials are used in the gate, stress effects on diffusion become a more prevalent component in determining the final dopant profile and subsequent device performance.

On the experimental side, contradictory results for the qualitative influence of stress on boron diffusion further motivate a fundamental investigation of stress-mediated diffusion: Whereas the measurements of Aziz *et al.* [4,5,6] suggest enhanced diffusivity under compressive pressure, other work finds retarded diffusion in that case [3,7,8,9,10].

Most theoretical work on stress-mediated diffusion assumes a hydrostatic state of stress in the substrate, which is of course only a special case of a general anisotropic stress field. Stresses caused by dislocations, deposition process, thermal and geometric effects all add to a complex stress state under a multi-layered gate stack. Additionally, a stress concentration typically exists at the gate edge caused by the peeling stress peak at the free edge of the gate stack [11,12,13]. The resulting stress concentration can produce stress magnitudes approaching the material strength even at low temperatures [13,14]. With reducing feature sizes, the gate itself acts as a stress concentrator directly affecting not only diffusion, but device work function and band gap, carrier mobility, junction leakage and hot-electron lifetime [15]. The high stress concentration at the gate edge has even been used in nanometer scale patterning of $CoSi_2$ by using stress engineering to control patterning down to 50 nm features [16]. Stress effects on mobility were shown to significantly modify drive current for both NMOS and PMOS devices [15,17].

On the theoretical side, the only fundamental treatment of diffusion in a general stress field is given in the work of Dederichs and Schroeder [18]. However, we found their derivation from microscopic lattice hops to be only a special case of a more general solution derived for the first time in this work [19]. In the following, the sign of stresses will follow a physics convention of positive for compression and negative for tensile.

2 EXAMPLE: STRESSED GATE

The detrimental effects of stress mediated diffusion for submicron devices became evident when investigating new exotic gate materials. Anomalous B diffusion, which appeared stress dependent, was discovered in a Motorola developed TiN metal-gate structure [17]. Electrically measured results indicated a decreasing L_{eff} (PMOS) with increasing TiN thickness in the SiO_2/TiN/Poly/SiO_2 gate stack. A finite element (FE) model of the gate stack was produced and used to predict stress values during the rapid thermal anneal experienced by the stack. Figure 1 shows an example scanning electron microscope (SEM) image of the gate along with the representative FE model. The resulting relation between measured L_{eff} and substrate stress as a function of TiN thickness can be seen in Fig. 2.

The qualitative agreement between the stress and diffusion results presented in Fig. 2 encouraged a further development of a stress-dependent diffusion methodology. The following work focuses on the effects of an externally applied stress tensor on the diffusion of B. The resulting

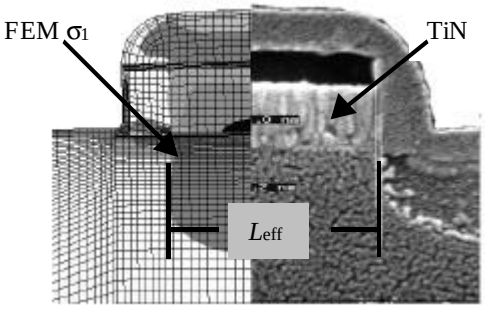

Fig. 1. SEM and FE model of the TiN gate stack [17].

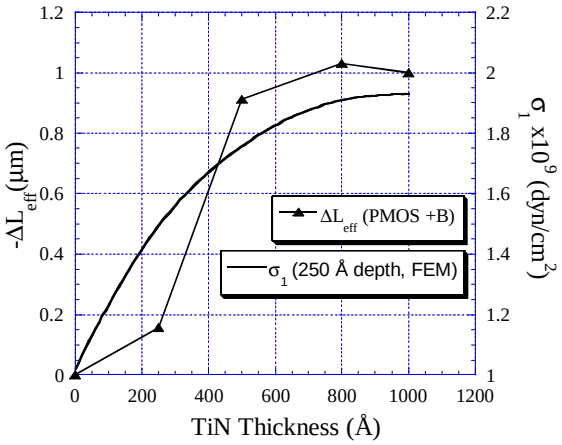

Fig. 2. ΔL_{eff} (measured) and σ_1 (FEM) versus TiN thickness. FE stress results are reported from 250 Å directly under the gate edge at a temperature of 1050 °C.

tool will be used to stress engineer submicron devices where features such as trench isolation, exotic gate materials, stressed substrates and shrinking device sizes all lead to drastic increases in substrate stresses and anomalous device performance.

3 BORON DIFFUSION MODEL

Boron has been found to diffuse nearly exclusively with the help of Si self-interstitials [20,21]. With the help of ab-initio calculations, we have recently found a new microscopic picture: Rather than diffusing over long distances by hopping between interstitial sites after being kicked out from a substitutional to an interstitial site, we find B to prefer to kick back in to a substitutional site right after the kick-out, resulting in a two-step diffusion mechanism that can be simply modeled by a mobile B*I* pair (see Fig. 3). The intermediate hexagonal interstitial is a saddle point for the positive, and a local minimum for the neutral charge state [20]. For the sake of simplicity, we assume it to be the saddle point for all charge states in *p*-Si.

We start from a standard four-stream diffusion model for B with the streams *I* (self-interstitials, mobile), *V* (vacancies, mobile), B (substitutional B, immobile), and B*I*

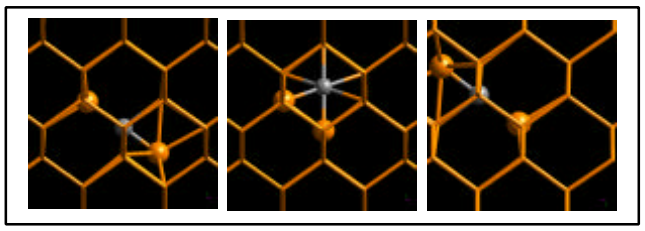

Fig. 3. Diffusion path for B as determined from ab-initio calculations [19]. The smaller ball is the B atom.

(B-interstitial pair, mobile) and use effective parameters according to the dominant charge states at mid gap [20] to keep the model as simple as possible. Assuming that the point-defects (*I* and *V*) are in equilibrium with a free surface and that the *I* concentration is independent of the B concentration, we can simplify the four stream model to an effective one-stream model

$$\dot{c}_{\mathrm{B}} = \nabla \cdot \left[\underline{\underline{P}}_{\mathrm{B}}^{\mathrm{eff}} \cdot \nabla \left(c_{\mathrm{B}} / S_{\mathrm{B}}^{\mathrm{eff}} \right) \right], \qquad (1)$$

where c_{B} is the B concentration, $\underline{\underline{P}}_{\mathrm{B}}^{\mathrm{eff}}$ is the effective solid permeability tensor and $S_{\mathrm{B}}^{\mathrm{eff}}$ is the solid solubility factor [19]. In the hydrostatic case where the stress tensor is given by $s = p\underline{\underline{\mathrm{Id}}}$, the permeability (which is a scalar now) as a function of the pressure p is given by

$$P_{\mathrm{B}}^{\mathrm{eff}} = P_{BI} = D_{\mathrm{B}I}^{0} \exp\left[-\left(e_{(s)}^{BI} + p\Omega_{(s)}^{BI} \right) / k_B T \right], \qquad (2)$$

where $D_{\mathrm{B}I}^{0}$ is the diffusivity prefactor for the B*I* pair which we calculate from first principles within the harmonic Vineyard method [22], $e_{(s)}^{BI}$ is the creation energy for the B*I* pair at the saddle point (given by the difference between the bare total energies of a supercell with B*I* at the saddle point and perfect Si in the equivalent cell), $\Omega_{(s)}^{BI}$ is the corresponding creation volume (volume difference instead of energy difference in above definition) [23], k_B is the Boltzmann constant, and T the temperature. For the solubility, we find

$$S_{\mathrm{B}}^{\mathrm{eff}} = \exp\left\{ -\left[e_{(v)}^{\mathrm{B}} + e_{\mathrm{at}} + p\left(\Omega_{(v)}^{\mathrm{B}} + \Omega_{\mathrm{at}} \right) \right] / k_B T \right\} / \left(4pC_I^0 \right), \qquad (3)$$

where $e_{(v)}^{\mathrm{B}}$ is the creation volume for substitutional B in its ground state or "valley", e_{at} is the total energy per atom of the perfect Si cell, $\Omega_{(v)}^{\mathrm{B}}$ is the corresponding creation volume for substitutional B, Ω_{at} the volume per atom of perfect Si, and C_I^0 the entropy prefactor for the equilibrium *I* concentration $C_I^* = C_I^0 \exp\left(-E_{\mathrm{form}} / k_B T \right)$ [23]. For the anisotropic case with general stress tensor, the expressions

are more complicated and will be given elsewhere [19]. In the general case, the pressure dependence is given by the respective creation volume tensors which are calculated by the length changes ΔL_a between the defective cell and the perfect Si cell with lattice parameters L_a ,

$$\underset{=}{\Omega} = \begin{pmatrix} L_y L_z \Delta L_x & 0 & 0 \\ 0 & L_z L_x \Delta L_y & 0 \\ 0 & 0 & L_x L_y \Delta L_z \end{pmatrix} \quad (4)$$

4 AB-INITIO RESULTS

Since most of the microscopic quantities in the pressure-dependent diffusion Eq. (1) are not accessible to experiment, we have calculated them from first principles. Although numerous ab-initio calculations examining the (scalar) pressure dependence of diffusion in the *hydrostatic* case have been performed in the past [24,25], there is to the best of our knowledge no report on the corresponding tensor dependence for the general anisotropic stress case in the literature.

For our ab-initio calculations, we used the plane-wave code VASP [26] within the general-gradient approximation. Special care was taken to minimize finite-size errors. From supercell calculations with up to 1000 atoms in the cell, we found especially that the finite-size change of the bulk modulus of the defective cell can strongly influence the results, an error that can be easily corrected for in small cells (with, e.g., 64 atoms). "Scissor" type corrections for band gap errors have also been applied; details can be found elsewhere [23].

For the energies required to evaluate Eq. (1), we find corrected values of $e^{\mathrm{B}}_{(v)} + e_{\mathrm{at}} = -7.14$ eV and $e^{BI}_{(s)} = -3.39$ eV which result in a net activation energy $E_a = -\left(e^{\mathrm{B}}_{(v)} + e_{\mathrm{at}}\right) + e^{BI}_{(s)} = 3.75$ eV in agreement with the experimental value of Ref. [27]. For the permeability and solubility volumes, we find in a principal-axis coordinate system

$$\underset{=}{\Omega}^{BI}_{(s)} = \begin{pmatrix} 9.5 & 0 & 0 \\ 0 & -3.8 & 0 \\ 0 & 0 & -3.8 \end{pmatrix} \text{Å}^3$$

(the principal axis for 9.5 Å^3 along the (111) direction) and

$$\underset{=}{\Omega}^{\mathrm{B}}_{(v)} + \underset{=}{\Omega}_{\mathrm{at}} = \begin{pmatrix} 2.4 & 0 & 0 \\ 0 & 2.4 & 0 \\ 0 & 0 & 2.4 \end{pmatrix} \text{Å}^3,$$

respectively, with scalar values for the hydrostatic case of $\mathrm{Tr}\left(\underset{=}{\Omega}^{BI}_{(s)}\right) = 1.9$ Å^3 and $\mathrm{Tr}\left(\underset{=}{\Omega}^{\mathrm{B}}_{(v)} + \underset{=}{\Omega}_{\mathrm{at}}\right) = 7.2$ Å^3. The net scalar activation volume V_a for B diffusion, which can be calculated from $V_a = -\mathrm{Tr}\left(\underset{=}{\Omega}^{\mathrm{B}}_{(v)} + \underset{=}{\Omega}_{\mathrm{at}}\right) + \mathrm{Tr}\left(\underset{=}{\Omega}^{BI}_{(s)}\right)$, is found to be –5.3 Å^3, in good agreement with recent experiments of –3.4 Å^3 [5] and an (isotropic) ab-initio calculation of –3.1 Å^3 [25]. Although the hydrostatic value is small, there is considerable anisotropy in the permeability volume tensor which can have a considerable effect on diffusion under anisotropic strain [19].

Our result means that in the equilibrium case that we consider, B diffusion is enhanced by compressive pressure. This could look counterintuitive at first glance, since one might expect interstitial diffusion to be retarded in a compressed lattice. In order to understand this pressure dependence of the B diffusivity better, it is helpful to first separate the activation volume into $V_a = V_I^{\mathrm{form}} + V_{BI}^{\mathrm{asso}} + V_{BI}^{\mathrm{mig}}$ [5]. From ab-initio calculations, we find $V_I^{\mathrm{form}} \approx -9$ Å^3 [20] for systems with interstitials interacting with free surfaces, which on the other hand results in $V_{BI}^{\mathrm{asso}} + V_{BI}^{\mathrm{mig}} \approx 4$ Å^3. Thus, the (strongly) negative value of V_I^{form} causes the overall B activation volume V_a to be negative despite the fact that binding and migration of B*I* pairs is retarded. If the interstitial, on the other hand, would not stem from a free surface, the overall interstitial concentration should be lower [20], resulting in a positive B activation volume, i.e., retarded diffusion under compressive pressure. Because nitride or other top layers inject defects and therefore modify the point defect concentrations, the surface conditions can influence the dependence of the diffusivity on pressure; this might explain the qualitative differences in experiments [4-10].

5 STRESS CALCULATIONS

Although stress effects on diffusion have been observed in advanced gate structures as described earlier [17], this paper considers a more basic example to demonstrate the developed predictive capability. A 1000 Å Si_3N_4 stripe $(0.25mm \times 5.0mm)$ on a Si (100) substrate is used. The stress field in the Si substrate at diffusion temperatures (1100 ^{o}C) is determined using FE methods. Since temperature dependence of elastic properties for most materials in a gate stack, except for Si, is unknown, empirical data is used to assist in bounding the high temperature stress simulations. Using a high temperature radius of curvature tool provided by FSM, Inc. [27], $\sigma(T)$ for a variety of materials on Si were measured. The global (full coverage) empirical stress data was used to define the high temperature stress values in feature scale simulations. Further details can be found elsewhere [28].

Full 3-D stress finite element (FE) models were required due to the configuration of the problem. The stressed area of interest is directly below the surface of the substrate near both the Si/Si_3N_4 interface and the traction-free boundary of open air. This proximity to the surface makes both plane-

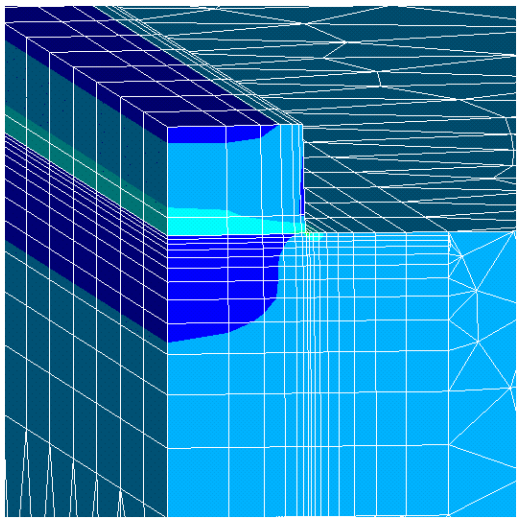

Fig. 4. Typical 3-D finite element model of a Si_3N_4 on Si substrate. *X*-direction (left-to-right) stress shown; compression under the stripe and tension just to the right of the stripe.

strain and plane-stress 2-D reductions incorrect and forces a full 3-D model to be used. Figure 4 shows the cross section of the quarter model developed in ANSYS^{TM} for a Si_3N_4 stripe on Si. A 100 Å SiO_2 film (not shown) was modeled over the Si/Si_3N_4 in order to reduced the potential singularity found in FE peeling stress results near free traction boundaries [29]. The tensile Si_3N_4 produces compressive *x*-direction stresses directly under the stripe and large compressive and tensile stress concentrations just under and outside the Si_3N_4 stripe edge, respectively. Resulting stress tensors from the FE model are passed through nodal data to an in-house stress diffusion solver.

6 CONTINUUM SOLVER

We have developed a new simulation tool for stress-mediated diffusion problems that is based upon the PDE solver described in [30]. This solver implements the gradient-weighted moving finite element method which uses a continuously moving mesh that adapts to the evolving solution. Instead of directly implementing (1) on our solver, it is useful for a number of mathematical reasons to first make a change of dependent variable $u = C_B / S_B^{\text{eff}}$. In this new variable (1) becomes $S_B^{\text{eff}} \partial u / \partial t = \nabla \cdot P_B^{\text{eff}} \nabla u$.

Because the concentration tail is as important as the high-concentration regions, we make a further change of variables, letting $w = \log(u)$. Thus the final equation that we implement on our solver is

$$S_B^{\text{eff}} \frac{\partial w}{\partial t} = \nabla \cdot P_B^{\text{eff}} \nabla w + \nabla w \cdot P_B^{\text{eff}} \nabla w \qquad (5)$$

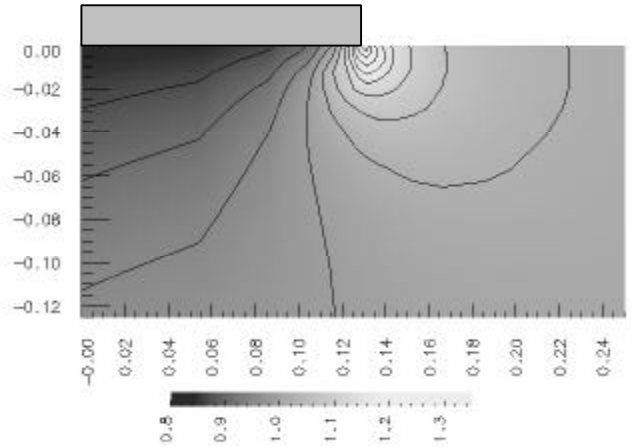

Fig. 5. Solubility S_B^{eff} for a 2-D cross section of the described 3-D stress state.

Other more sophisticated stretching transformations, which interpolate between u and $\log u$, can be used instead. Our Galerkin equations are obtained by minimizing the residual of this equation with respect to a $1/S_B^{\text{eff}}$ weighted L^2 norm (see [30] for details of this procedure).

At present the stress tensor, upon which S_B^{eff} and P_B^{eff} depend, is simply obtained by interpolating the stress field computed by ANSYS onto the moving mesh used in our solver. We are currently developing a first-order system least squares (FOSLS) solver for the equations of thermoelasticity that will couple directly to our diffusion solver and replace the input from ANSYS. This FOSLS solver will directly approximate the stress tensor using a continuous piecewise linear finite element space over the same moving mesh (or refinement thereof), providing a more accurate stress solution and eliminating the need for interpolation.

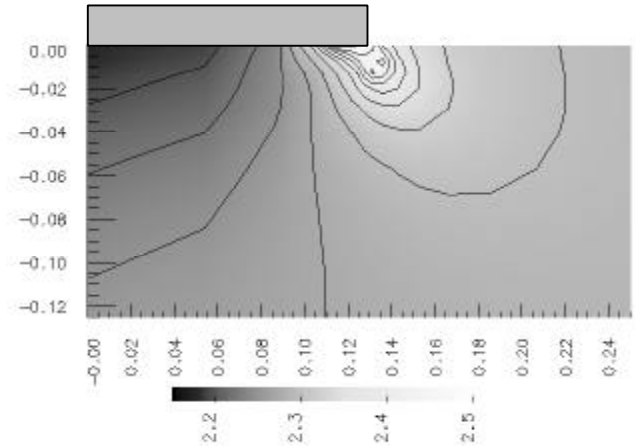

Fig. 6. Permeability (*yy*-component) P_B^{eff} for a 2-D cross section of the described 3-D stress state.

In Figs. 5 and 6, we show S_B^{eff} and P_B^{eff} in a 2-D cross-section of the 3-D stress calculation described in Sec. 5. We find already for this system with very small and isotropic stresses, in contrast to metal-gate systems, a change in the overall diffusivity of tens of percent. Application of this tool-set to stress mediated diffusion issues such as trench isolation, SOI, short channel effects and advanced gate design will be addressed elsewhere.

7 CONCLUSIONS

We have demonstrated for the first time the development of a complete methodology to simulate the effects of general anisotropic non-uniform stress on diffusion of B in Si. The macroscopic diffusion equation has been derived from microscopic transition state theory, relating the diffusivity to the microscopic jump parameters. We have derived from a detailed knowledge of the microscopic processes and the interactions between point defects and B atoms a simple one-stream model, which describes the intrinsic B diffusion in the presence of non-uniform anisotropic stress. The required microscopic parameters have been calculated from first principles, for the first time in their full tensor form. Furthermore, we have measured the stress in the gate stack materials as a function of temperature and used it to develop a stress-prediction methodology. These capabilities and numbers were finally combined implemented into a continuum model and used to examine diffusion in the stress field of a nitride stripe. For the investigated case, small isotropic stresses were predicted (in contrast to the metal gate example). Even with these small stress variations, overall diffusivity was found to vary a few tens of percent across the simulated domain.

ACKNOLWEDGMENTS

We would like to thank Bikas Maiti from Motorola for many beneficial discussions and for providing the presented experimental L_{eff} data. We additionally thank Mike Aziz from Harvard for very helpful discussions throughout this work.

REFERENCES

[1] P. Kuo, Appl. Phys. Lett. **66**, 580 (1995).
[2] Y. Zaitso *et al.*, Mater. Sci. Forum **196-201**, 1891 (1995).
[3] H. Park *et al.*, J. Appl. Phys. **78**, 3664 (1995).
[4] M. Aziz, Defect and Diffusion Forum **153-155**, 1 (1998); Y. Zhao, M. Aziz, S. Mitha and D. Schiferl, Appl. Phys. Lett.74, **31-33** (1999).
[5] Y. Zhao, M. Aziz, H-J. Gossmann, S. Mitha, and D. Schiferl, Appl. Phys. Lett. **75**, 941 (1999).
[6] Y. Zhao, M. Aziz, H. J. Gossmann, and S. Mitha, Appl. Phys. Lett. **74**, 31 (1999).
[7] S. Chaudhry and M. Law, J. Appl. Phys. **82**, 1138 (1997).
[8] K. Osada *et al.*, J. Electrochem. Soc. **142**, 202 (1995).
[9] Y. Todokoro, J. Appl. Phys. **49**, 3527 (1978).
[10] S. Chaudhry and M. Law, J. Appl. Phys. **82**, 1138 (1997).
[11] E. Suhir, J. Appl. Mechanics **55**, 143 (1988).
[12] B. Gu and P.E. Phelan, Applied Superconductivity **6**, 19 (1998).
[13] D. B. Bogy, "Edge-Bonded Dissimilar Orthogonal Elastic Wedges Under Normal and Shear Loading", Transactions of the ASME, pp. 460-466, Sept. 1968.
[14] C. Chung and J.W. Eischen, Int. J. Solids Structures **28**, 105 (1991).
[15] G. Scott, J. Lutze, M. Rubin, F. Nouri, and M. Manley, "NMOS Drive Current Reduction Caused by Transistor Layout and Trench Isolation Induced Stress", IEDM, Session 34, 1999.
[16] Q.T. Zhao, F. Klinkhammer, M. Dolle, L. Kappius and S. Mantl, Appl. Phys. Lett. **74**, 454 (1999).
[17] B Maiti *et al.*, "PVD TiN Metal Gate MOSFETs on Bulk Silicon and Fully Depleted Silicon-On-Insulator (FDSOI) Substrates for Deep Sub-Quarter Micron CMOS Technology", IEDM, Session 29, 1998.
[18] P. H. Dederichs and K. Schroeder, Phys. Rev. B **17**, 2524 (1978).
[19] M. S. Daw, W. Windl, M. Laudon, N.N. Carlson, and M. P. Masquelier (unpublished).
[20] W. Windl, M. M. Bunea, R. Stumpf, S. T. Dunham, and M. P. Masquelier, Proc. MSM 99, (Cambridge, MA, 1999), p. 369; Phys. Rev. Lett. **83**, 4345 (1999).
[21] A. Ural, P. B. Griffin, and J. D. Plummer, Phys. Rev. Lett. **83**, 3454 (1999).
[22] B. P. Uberuaga, R. Stumpf, W. Windl, H. Jonsson, and M. P. Masquelier (unpublished).
[23] W. Windl, M. S. Daw, M. Laudon, N. N. Carlson, and M. P. Masquelier (unpublished).
[24] See, e.g., A. Antonelli and J. Bernholc, Phys. Rev. B **40**, 10643 (1989); A. Antonelli, E. Kaxiras, and D. J. Chadi, Phys. Rev. Lett. **81**, 2088 (1998).
[25] B. Sadigh *et al.*, Phys. Rev. Lett. **83**, 4341 (1999).
[26] G. Kresse and J. Hafner, Phys. Rev. B **47**, RC558 (1993); G. Kresse and J. Furthmüller, Comput. Mat. Sci. **6**, 15 (1996); Phys. Rev. B **54**, 11169 (1996).
[27] B. Folmer, Y. M. Haddara, and M. E. Law (unpublished).
[27] S.H. Lau, Private communication, Frontier Semiconductor Measurement, Inc., San Jose, CA, (1999)
[28] M. Laudon, N.N. Carlson, M. S. Daw, W. Windl, and M. P. Masquelier (unpublished).
[29] B. Gu and P.E. Phelan, J. Appl. Superconductivity **6**, 19 (1998).
[30] N. N. Carlson and K. Miller, SIAM J. Sci. Computing **19**, 728 (1998); *ibid.*, 766 (1998).